JOURNAL OF CATALYSIS **168,** 164–175 (1997)
ARTICLE NO. CA971621

Pt/Al_2O_3 Catalysts and $Pt–Sn/Al_2O_3$ Catalysts Prepared by Two Different Methods: Hydrogen Pressure Effects in the Reactions of *n*-Hexane

Z. Paál,* A. Győry,* I. Uszkurat,*,[1] S. Olivier,† M. Guérin,† and C. Kappenstein†

*Institute of Isotopes of the Hungarian Academy of Sciences, PO Box 77, H-1525 Budapest, Hungary; and †LACCO, URA CNRS 350, Faculté des Sciences, Université de Poitiers, 40 Avenue du Recteur Pineau, 86000 Poitiers, France

Received February 7, 1996; revised December 10, 1996; accepted January 20, 1997

$Pt–Sn/Al_2O_3$ catalysts were prepared using two different methods, namely, by "traditional" coimpregnation with H_2PtCl_6 and $SnCl_4$ and by a "new" method in which the bimetallic complex precursor $[Pt(NH_3)_4][SnCl_6]$ is prepared on the support. Their catalytic activity and selectivity in *n*-hexane reactions were studied as a function of the hydrogen pressure (60–480 Torr) and compared with those of monometallic Pt/Al_2O_3 catalysts using H_2PtCl_6 or $[Pt(NH_3)_4]Cl_2$ as Pt precursors. Pt/Al_2O_3 ex $[Pt(NH_3)_4]Cl_2$ showed very low dispersion and exhibited high selectivity in reactions attributed to multiatomic ensembles. The results with bimetallic catalysts can be rationalized in terms of two phases being present, a PtSn alloy phase plus Pt in fine distribution. The "new" $Pt–Sn/Al_2O_3$ from the bimetallic precursor contains the two metals in a better dispersion, resulting in a larger number of atomically dispersed surface Pt active sites. This catalyst gave more isomers (and methylcyclopentane) and fewer fragments and less benzene than the "traditional" sample. The "new" $Pt–Sn/Al_2O_3$ sample possessed good long-term stability. The "traditional" sample lost some of its activity and its high hydrogenolysis selectivity during long use; i.e., it approached the catalytic properties of the "new" sample. Both samples are potential candidates as catalysts with high isomerizing and low aromatic selectivities (up to 75% isohexanes plus methylcyclopentane as opposed to a maximum of 20% benzene). The results could be explained sufficiently with a geometric model, electronic interactions playing a less important role in the catalytic phenomena observed.

© 1997 Academic Press

INTRODUCTION

A number of promoter metals (e.g., Re, Sn, Ir) have been used as additives for naphtha reforming Pt catalysts to increase catalyst lifetime by hampering coking and/or to improve selectivity of desired products (1, 2). Some of the additives have catalytic properties on their own (Re, Ir) while others are catalytically inactive (Sn). Tin added to Pt catalysts for naphtha reforming may be a good candidate for shifting the reforming selectivity toward nondegradative products, in particular, isomerization, rather than to the production of aromatics, which become undesirable components in commercial naphtha.

Sn can modify the stability and selectivity of the Pt function in two ways (3–13):

1. By an "ensemble effect": Tin decreases the number of contiguous platinum atoms, tin atoms dividing the platinum surface into smaller ensembles (1). By doing so, multipoint adsorption of hydrocarbon molecules on the surface is hampered; thus, hydrogenolysis and deactivation by coke deposition can be reduced (4–8);
2. By an "electronic effect": Tin changes the electronic environment of Pt atoms (1–13). Parera *et al.* (13) proposed that this type of interaction between Pt and the additive results in more electron-deficient Pt atoms, which influence markedly the adsorption–desorption steps of the catalytic reaction.

The proper explanation of the role of tin in $Pt–Sn/Al_2O_3$ catalysts is closely related to the chemical state of Sn. Both are still under debate. It is likely that the results reported so far depend also on the catalyst preparation, pretreatment, experimental techniques applied, and parameters studied. One has to recall the statement of Burch and Garla that there is no geometric effect without electronic interaction (11). This statement is in agreement with the results of Palazov *et al.* (14), who also concluded that both electronic and geometric effects are important and were in close relationship in $Pt–Sn/Al_2O_3$ catalysts.

Biloen *et al.* (15–17) examined the role of second metals added to Pt in *n*-hexane conversion. Tin increased the stability of the catalyst and reduced coke deposition. Temperature-programmed reduction (TPR) studies suggested that the zero-valent Pt and Sn atoms formed during reduction are in intimate contact and pointed to the presence of true platinum–tin alloys or bimetallic clusters. The catalyst was not homogeneously alloyed: it contained free Pt and Pt-rich and Sn-rich alloys as well (16). They put forward the ensemble model based on the rather drastic changes observed in the selectivity: tin would act accordingly by

[1] On leave from Fachhochschule Ostfriesland, D-26723 Emden, Germany.

0021-9517/97 $25.00
Copyright © 1997 by Academic Press
All rights of reproduction in any form reserved.

dividing the platinum surface of Pt/alumina and Pt/SiO_2 catalysts into ensembles of one to three platinum atoms (15). Their basic explanation for the ensemble effect was that alloying Pt with Sn suppresses all the reactions that require relatively large Pt ensembles, but it does not affect (de)hydrogenation, which Biloen *et al.* (17) attributed to monoatomic active sites.

Burch and Garla (10, 11) stated that Sn(IV) was reduced only to Sn(II). They attributed the altered Pt properties to a change in the electronic properties of small Pt crystallites containing Sn(II) stabilized by its interaction with alumina or to a few percent of metallic Sn incorporated as a solid solution in Pt rather than as an intermediate stoichiometric alloy (18).

Some X-ray photoelectron spectroscopy (XPS) studies pointed to the presence of tin predominantly in the oxidized state in $Pt–Sn/Al_2O_3$ (19–21). On $Pt–Sn/SiO_2$, however, large amounts of Sn^0 were present (21). A tin aluminate eggshell surrounding the Al_2O_3 particles was suggested as the support of Pt particles (19). Li *et al.* (22, 23) reported that a portion of tin was present in the Sn^0 state but they could not prove the presence of PtSn alloys; however, the same group detected the presence of an intermediate PtSn alloy with a stoichiometry of Pt/Sn = 1 : 1 by *in situ* X-ray diffraction (XRD) (24). Mössbauer studies (25–28) provided evidence for the formation of PtSn alloys and highly dispersed particles containing Sn in the +IV, +II and zero states. In addition to Sn–O–Pt bonds (21), the role of $Sn–Cl–Al_2O_3$ interactions was stressed (27). A catalyst preparation method using a surface reaction between Pt–H and tin alkyls was found to produce predominantly Pt_xSn alloys (28). Srinivasan and Davis (29) studied the phase composition of 1% Pt/SiO_2 with increasing amounts of Sn added and found alloy formation with Sn exceeding the ratio Pt : Sn = 3 : 8 only. No single structure could be ascribed to all catalysts with various Pt : Sn ratios.

Lieske and Völter (30) studied $Pt–Sn/Al_2O_3$ catalysts (0.5 and 1.0 wt% Pt, 0.3–1.2 wt% Sn), by using TPR and adsorption of oxygen and hydrogen. Their main conclusion was the coexistence of Sn in various chemical states: a minor part of tin was reduced from +IV to the zero state and this latter one formed an alloy with Pt. The major part of the tin was reduced to a +II state which was stabilized by alumina. The PtSn alloy formed two-dimensional clusters on the alumina surface, surrounded by Sn(II) species. The amount of alloyed tin as well as the percentage of Sn in the alloy phase increased with increasing total tin content.

Joyner and Shpiro (31) proposed that the surface monolayer of the active particles should consist of platinum, the additive being located in the immediate subsurface layer, where its concentration will be enriched. The primary influence on Pt properties would accordingly be an electronic interaction between these two layers, as opposed to the "ensemble" or "ligand effects" (3). In this case the hydrogen adsorption ability of Pt with a tin underlayer should decrease.

Earlier we reported (32) differences in physical and catalytic properties between $Pt–Sn/Al_2O_3$ samples prepared by using different precursors. Catalyst **T** was prepared by "traditional" coimpregnation and catalyst **N** by using a new precursor, $[Pt(NH_3)_4][SnCl_6]$. The formation of this bimetallic precursor could be proven by indirect methods only. Its platinum analog, the green Magnus salt $[Pt(NH_3)_4][PtCl_4]$, was formed on alumina support when the complex cation was introduced first, since when $[PtCl_4]^{2-}$ anion was introduced first, it rapidly exchanged its Cl ligands with O in the support (33a). The same was observed when one Pt was replaced by Ir (33a). The interaction of $SnCl_4$ with alumina is much more rapid and competes with its interaction with the platinum cation. Nevertheless, EXAFS studies provided indirect evidence for the formation of the bimetallic complex precursor of catalyst **N** (33b). Reduction produced a mixture of Pt clusters and some PtSn alloys. Near the Pt clusters tin was in the zero oxidation state covered with tin oxides and traces of chlorine.

Catalysts from different precursors were also probed by other experimental techniques:

—TPR studies showed a deeper tin reduction for catalyst **N**.

—Microscopic examinations revealed larger crystallite size for catalyst **N**.

—*Ex situ* XRD performed with samples containing higher loading (2 wt% Pt and atomic Pt/Sn ratio = 1/1) displayed the presence of a stoichiometric PtSn alloy (33b).

—Catalytic measurements showed higher turnover frequency (TOF) values for ring opening of cyclopentane and dehydrogenation of cylohexane over catalyst **T** than on catalyst **N** (32).

As a conclusion of both structural and catalytic studies, a more intimate contact between Pt and Sn atoms seemed to determine the structure and activity of the centers of catalyst **N** reduced from a bimetallic complex precursor. Further studies (33c), including Mössbauer spectroscopy, XRD, EXAFS, and temperature-programmed methods of a similar sample, confirm this statement.

The present study reports detailed results on both catalysts, mainly on the effect of hydrogen pressure on catalytic properties in skeletal reactions of *n*-hexane. These catalysts are compared with monometallic Pt/Al_2O_3 samples prepared using the same platinum precursors as in the preparation of bimetallic ones. The main tool to be used is the catalytic runs as a test method to be able to probe the active centers themselves. Skeletal reactions of *n*-hexane include isomerization, C_5 cyclization, aromatization, and hydrogenolysis and are accompanied by dehydrogenation to hexenes (34). The selectivity of these reactions can be characteristic of the active ensembles

available and their relative importance depends also on the hydrogen pressure (35, 36). A well-characterized (37) standard Pt/SiO_2 catalyst, EUROPT-1, was used for comparison.

EXPERIMENTAL

Catalysts

One of the Pt–Sn/alumina catalysts (**N**) was prepared by wetness impregnation using a new bimetallic precursor, $[Pt(NH_3)_4][SnCl_6]$, prepared in the pores of the support [cubic γ-alumina, Rhone–Poulenc GFS-400, see also in Ref. (32)]. The impregnation procedure involved two steps: the alumina was impregnated in the first step with $Pt(NH_3)_4Cl_2 \cdot H_2O$ and in the second step, with $SnCl_4 \cdot 5H_2O$ in HCl solution. After each step it was dried at 353 K and finally overnight at 393 K in an oven. The other catalyst (**T**) was produced with the traditional coimpregnation technique using a mixture of H_2PtCl_6 and $SnCl_4$. After drying, the impregnated alumina was left overnight at 393 K in an oven.

The effect of tin was examined by comparing the $Pt–Sn/Al_2O_3$ catalysts with Pt/Al_2O_3 samples prepared with the same platinum compounds as the precursors (**PN** for $Pt(NH_3)_4Cl_2 \cdot H_2O$ and **PT** for H_2PtCl_6, respectively).

Catalyst Characterization

Table 1 summarizes some characteristics of these catalysts. Platinum dispersion was determined by hydrogen chemisorption (HC) and also by oxygen titration (OC) and hydrogen titration (HT) using H_2 and O_2 pulses. The HC/OT/HT stoichiometry was 1/1.5/3. Both chemisorption and titration results gave the same dispersion value. As the relative error of titration was smaller, its values were used for TOF calculations. Excess oxygen consumption indicated slow oxidation of the oxidizable tin component; hence, stabilized stoichiometry was reached only after a few O_2–H_2 cycles. The stabilized values could be attributed to the oxygen–hydrogen chemisorption occurring only on the Pt component. Results obtained at 393 K agreed with those determined at room temperature. A TPR study of a sample with 1.5% Pt loading (Pt : Sn atomic ratio 1 : 1) to be reported separately (33c) showed that most of the reduction was completed up to 573 K. Tin was not reduced completely in this procedure.

TABLE 1

Characterization of the Catalysts

Catalyst	Type	Pt (wt%)	Sn (wt%)	Dispersion (%)
EUROPT-1	Pt/SiO_2	6.3	0	60[a]
PN	Pt/Al_2O_3	1.00	0	~1.3
PT	Pt/Al_2O_3	1.00	0	43.5
N	$Pt–Sn/Al_2O_3$	0.48	0.31	18.3
T	$Pt–Sn/Al_2O_3$	0.52	0.24	60.6

[a] This value measured in the present experiments agrees well with the widely accepted value for EUROPT-1, although some measurements from the original Eurocat group were higher, up to 100%. See review in Ref. (37).

Catalytic Runs

The reactions of *n*-hexane were studied in a closed circulation loop reactor with a volume of ~200 ml (35). The catalysts were first heated to 623 K (~20 K/min) in circulating H_2 at 120 Torr and were kept there for 1 h using a liquid nitrogen-cooled trap to freeze out water given off during removal of any oxygen from the catalyst surface. The loop was then evacuated and filled with a mixture of 10 Torr *n*-hexane reactant and hydrogen at different pressures (60, 120, 240, 360, or 480 Torr). The overall activity and product composition at 603 K were the same before and after runs at higher temperatures; hence, any marked changes of catalytic properties on heating and cooling in H_2 can be excluded.

Samples were taken mostly after 5 min reaction time but runs up to 240 min were also carried out. The temperatures of the reactions were 603 and 663 K. After the run was completed, the catalysts were regenerated at reaction temperature by the following procedure: evacuation, circulating air (100 Torr, 3 min), evacuation, and introduction of H_2 (100 Torr, 10 min). This treatment was carried out before starting the experiments every day, at the corresponding reaction temperature.

Analysis

Products (from methane up to benzene) were analyzed with a 50-m CP-Sil 5 glass capillary column.

Data Processing

When processing catalytic results, the product yields were calculated directly from analysis results. By normalizing them to total conversion = 100%, we obtained the product distribution. Selectivities were corrected for the mole number increase for fragments, i.e., expressed as moles of *n*-hexane transformed. Selectivities were also plotted as a function of conversion (35, 38). We also calculated the number of converted moles of *n*-hexane. Relating this value to unit mass Pt, overall activities were obtained. Rates were obtained by dividing the amount of hexane consumed by the length of the run. This time average was also used in longer runs rather than the more correct integration of differential rates. Specific activities (molecules per unit surface Pt per hour, i.e., TOF values) were calculated the same way and were related to the number of surface Pt atoms, as determined from the above dispersion values.

RESULTS

1. Monometallic Pt Catalysts: Pt/Al_2O_3 and EUROPT-1

These catalysts were compared at 603 K. Higher hydrogen pressures gave higher overall activity values (Fig. 1) on all catalysts studied. The overall activity of catalyst **PT** is the highest, but those of catalysts **PN** and **T** are close to it. The yields were in most cases around 10 to 15%, the maximum not exceeding 35%. Even in this latter case, *n*-hexane pressure dropped to 6.5 Torr from the initial 10 Torr. This difference between the initial and final pressures was not considered as influencing the time averaging markedly. TOF values calculated from dispersion data (Table 1) are shown in Fig. 2, omitting catalyst **PN** where these data must be rather uncertain due to the very low dispersion measured.

The yields on both catalysts increased at higher hydrogen pressures and remained in the same range (see caption to Fig. 3). Catalyst **PN** showed much lower hydrogenolysis selectivity than catalyst **PT** (Fig. 3). The selectivity of isomers increased at higher hydrogen pressures at the expense of methylcyclopentane on both Pt/Al_2O_3 catalysts. This agrees well with previously reported experience with EUROPT-1 (35, 36). Most benzene was produced at low hydrogen pressures, as also on EUROPT-1 and Pt-black (36). At higher hydrogen pressures catalyst **PN** (with the largest crystallites) exhibited higher aromatization selectivity (26–16%, as opposed to 18–12% on **PT**), and hydrogenolysis also was more pronounced on **PT** (up to 50% vs up to 30% on **PN**).

Increasing the hydrogen pressure caused a monotonic decrease in alkene selectivity over all Pt catalysts, dehydrogenation becoming insignificant at higher hydrogen pressures. Catalyst **PT** had slightly higher dehydrogenation selectivity at low hydrogen pressures than **PN**.

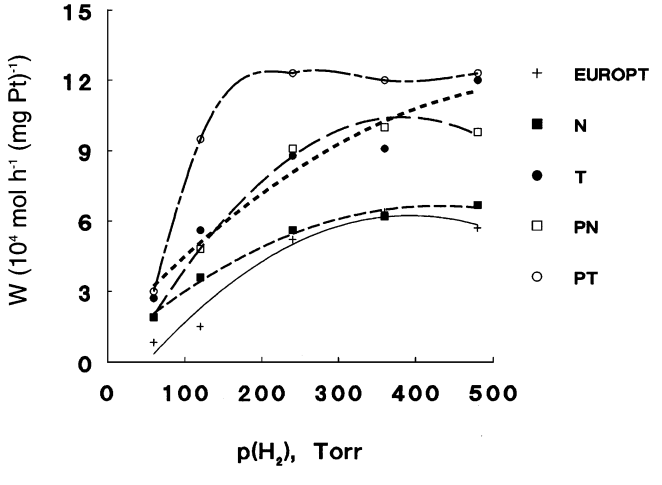

FIG. 1. Overall activity (moles of haxane transformed per unit mass Pt per hour) as a function of hydrogen pressure. $T = 603$ K.

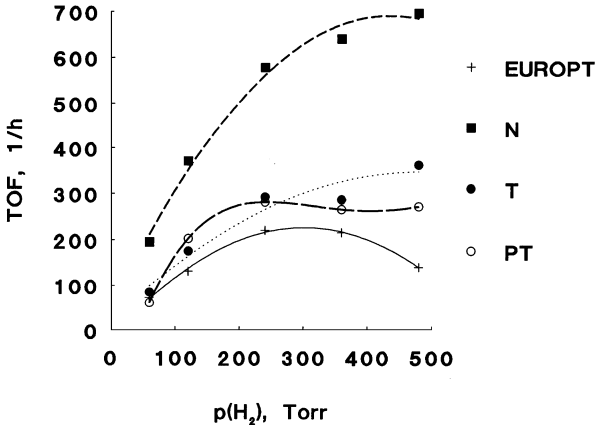

FIG. 2. Turnover frequency (molecules of haxane transformed per surface Pt atom per hour) as a function of hydrogen pressure. $T = 603$ K.

2. Pt–Sn/Al_2O_3 Catalysts

2.1. Activity and selectivity. Adding tin to Pt/alumina decreased the overall activities (Fig. 1) as compared with the parent monometallic sample (**T** vs **PT** and **N** vs **PN**). On the other hand, TOF values of the bimetallic samples were slightly above the analogous values for monometallic supported Pt catalysts (Fig. 2).

Plotting the selectivities as a function of overall conversion (38) should reflect their changes with progressing reaction, i.e., should reveal the formation of secondary products. Figure 4 shows that primary alkenes were transformed in further reactions, mainly to aromatics but other products are not excluded. The formation of isomers from methylcyclopentane is another secondary reaction; otherwise the selectivities are fairly stable within a rather wide range of conversion.

Based on this observation, we trust that plotting selectivities as a function of hydrogen pressure at constant sampling time (5 min) can give reliable information on their hydrogen pressure dependence (Fig. 5). The overall conversion increased more steeply when $p(H_2)$ increased from 60 to 120 Torr. A further $p(H_2)$ increase caused a slower increase in *n*-hexane consumption (see *W* values in Fig. 1, strictly proportional to the conversion).

The hydrogenolysis selectivity of $Pt–Sn/Al_2O_3$ catalysts was much lower than that of monometallic Pt catalysts. Higher hydrogen pressures enhanced hydrogenolysis markedly on Pt catalysts, but fragmentation selectivity increased only slightly with hydrogen pressures on both Pt–Sn samples. These latter samples produced more isomers and methylcyclopentane. The selectivity curves of isomers and MCP cross over with all catalysts. Of individual isomers, methylpentanes (MP) were present in the largest amount together with a small fraction of 2,3-dimethylbutane (2,3-DMB). The low values of the ratio 2,3-DMB/MP decreased with increasing hydrogen pressure (Table 2). At the same time, the ratio 2-MP/3-MP increased, approaching and even

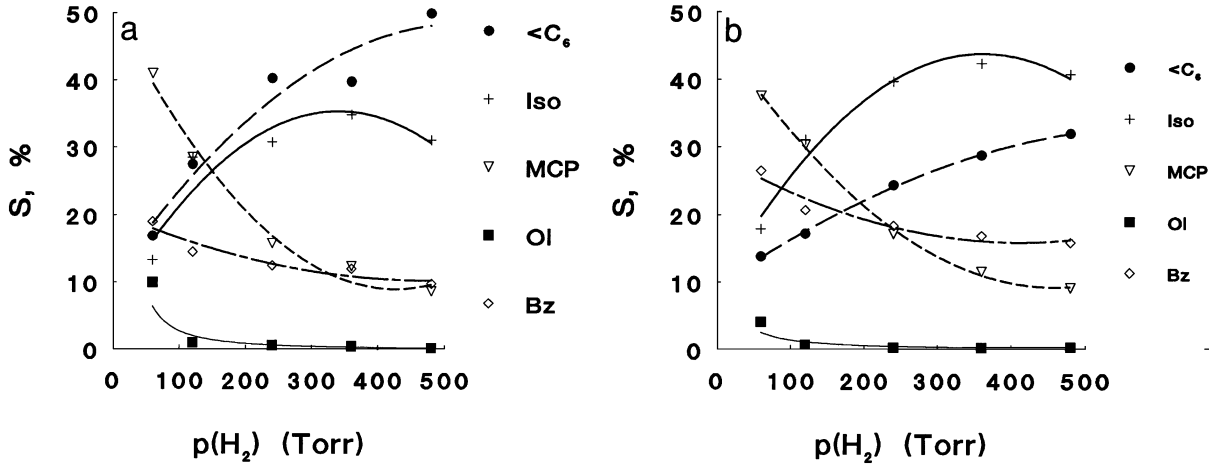

FIG. 3. Selectivities of individual products from *n*-hexane as a function of the hydrogen pressure on monometallic Pt/Al_2O_3 catalysts at $T = 603$ K. (a) Catalyst **PT** ("traditional"). Overall conversions: ~5% at $p(H_2) = 60$ Torr, ~16 to ~22% at higher hydrogen pressures. (b) Catalyst **PN** ("new"). Overall conversions: ~3% at $p(H_2) = 60$ Torr, ~8 to ~18% at higher hydrogen pressures.

exceeding the value of 2 (Table 3). Both values were rather similar to those observed over EUROPT-1. The aromatization selectivity of catalyst **N** is also inferior to that of sample **PN**. On catalyst **T**, on the other hand, more benzene was formed than on catalyst **PT**. More benzene was formed at low hydrogen pressures over all Pt/Al_2O_3 and $Pt–Sn/Al_2O_3$ catalysts, the lowest and highest selectivities differing by a factor between 1.5 and 2. Olefin production became insignificant at increasing hydrogen pressures over all catalysts.

The distribution of fragments obtained on both $Pt–Sn/Al_2O_3$ catalysts is shown in Fig. 6 (total amount of products formed = 100%). Catalyst **N** produced a rather pronounced methane excess at all hydrogen pressures. Much lower maxima are seen at C_3 and C_5 and the relative amount of all fragments is rather insensitive to hydrogen pressure. Catalyst **T**, in turn, gave more fragments but the corresponding amounts of C_1 and C_5 were much closer and a significant amount of propane was also formed. Splitting to give $C_2 + C_4$ was not favored at any hydrogen pressure.

2.2. Long-term activity and selectivity patterns. Continuing the runs for ca. 4 h, the selectivity of benzene, isomers, and fragments increased. More fragments and benzene were produced over sample **T**, as opposed to more pronounced MCP and isomer formation on catalyst **N**. Results obtained at 603 K are shown in Table 4. Isomers and fragments are also formed from primary products (such as methylcyclopentane), whereas olefins transform to give benzene. Aromatics and fragment selectivities were somewhat higher and that of saturated C_6 products lower on monometallic Pt/Al_2O_3 samples prepared with the "new" precursor (**PN** and **N**).

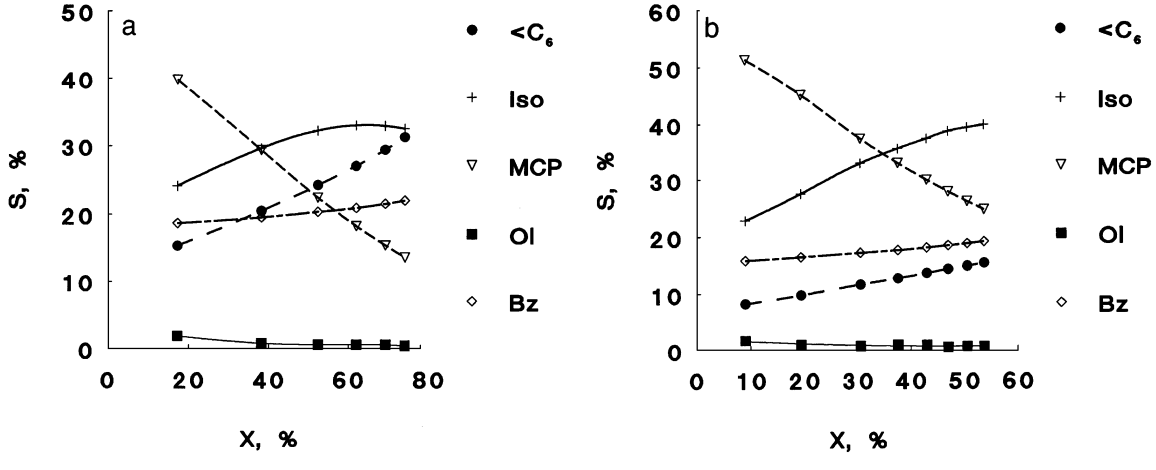

FIG. 4. Selectivity of individual product groups (S) as a function of overall conversion (X). $T = 603$ K, $p(nH) = 10$ Torr, $p(H_2) = 120$ Torr. (a) Catalyst **T**. (b) Catalyst **N**.

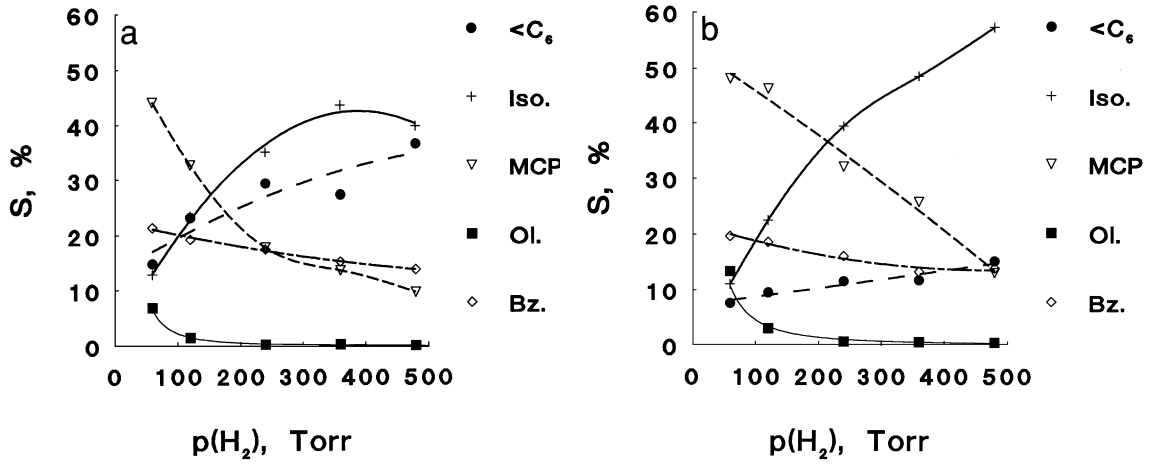

FIG. 5. Selectivities of individual products from *n*-hexane as a function of the hydrogen pressure on bimetallic Pt–Sn/Al_2O_3 catalysts at $T = 603$ K. (a) Catalyst **T** ("traditional"). Overall conversions: ~13% at $p(H_2) = 60$ Torr, ~19 to ~36% at higher hydrogen pressures. (b) Catalyst **N** ("new"). Overall conversions: ~5% at $p(H_2) = 60$ Torr, ~11 to ~18% at higher hydrogen pressures.

Several deactivation + regeneration cycles decreased the overall activity of catalyst **T** to a higher extent than that of catalyst **N** (Fig. 7, Table 5). Parallel to a rather marked drop in the overall conversion, the selectivities were also shifted after several regenerations. The direction of selectivity changes was the same with both catalysts (Table 5). The relative changes, however, were markedly different: catalyst **T** lost much more of its originally high fragmentation activity and approached the selectivity pattern of catalyst **N** after a few dozen regenerations. Benzene selectivity was rather stable and the sum of C_6 saturated products increased slightly at the expense of fragments.

The runs between the test measurements shown in Table 5 included several experiments with various durations, hydrogen pressures, and temperatures; they are the results presented in various tables and figures.

3. *Temperature Effects on Selectivities*

Our earlier publication (32) revealed that most marked differences between the activities of the two preparation methods were observed at higher reaction temperature. To complement the experiments reported earlier at one sampling time, we plotted the selectivity vs conversion (S–X) curves (38) at this higher temperature, too. Figure 8 shows olefins as probably the most abundant primary products, together with MCP, benzene, and, probably, fragments (even though no low conversion value could be presented with catalyst **T**). Fragments and benzene may have been formed in secondary reactions, too. Isomers also decompose (mainly to fragments) at large conversions, $X > 60\%$. The hydrogenolysis pattern after 100-min runs were rather similar to those shown in Fig. 6 for catalysts **T** and **N**, respectively.

The selectivities as a function of hydrogen pressure at 663 K on both monometallic and bimetallic samples are shown in Fig. 9. Raising the temperature enhanced benzene and olefin selectivities. The monometallic catalyst of the "new" preparation showed the highest aromatization ability, parallel with the lowest hexene formation. The fragment selectivity was surprisingly low over both Pt–Sn/Al_2O_3 samples. Isomer and MCP selectivities did not increase. MCP on bimetallic catalysts was the only product showing

TABLE 2

Ratio of 2,3-Dimethylbutane/Sum of Methylpentanes[a]

Catalyst	T (K)	$p(H_2)$ (Torr) 60	120	240	360	480
EUROPT-1	603	0.08	0.04	0.04	0.01	0.01
N	603	0.07	0.03	0.01	0.007	0.005
	663	0.16	0.12	0.08	0.07	0.03
T	603	0.10	0.05	0.03	0.01	0.01
	663	0.18	0.16	0.10	0.05	0.04

[a] Sampling time = 5 min, p(*n*-hexane) = 10 Torr.

TABLE 3

Ratio of 2-Methylpentane/3-Methylpentane[a]

Catalyst	T (K)	$p(H_2)$ (Torr) 60	120	240	360	480
EUROPT-1	603	1.47	1.82	2.10	2.26	2.31
N	603	1.44	1.84	2.07	2.18	2.25
	663	1.31	1.28	1.44	1.30	1.60
T	603	1.47	1.76	1.87	2.00	2.00
	663	1.31	1.20	1.44	1.56	1.60

[a] Sampling time = 5 min, p(*n*-hexane) = 10 Torr.

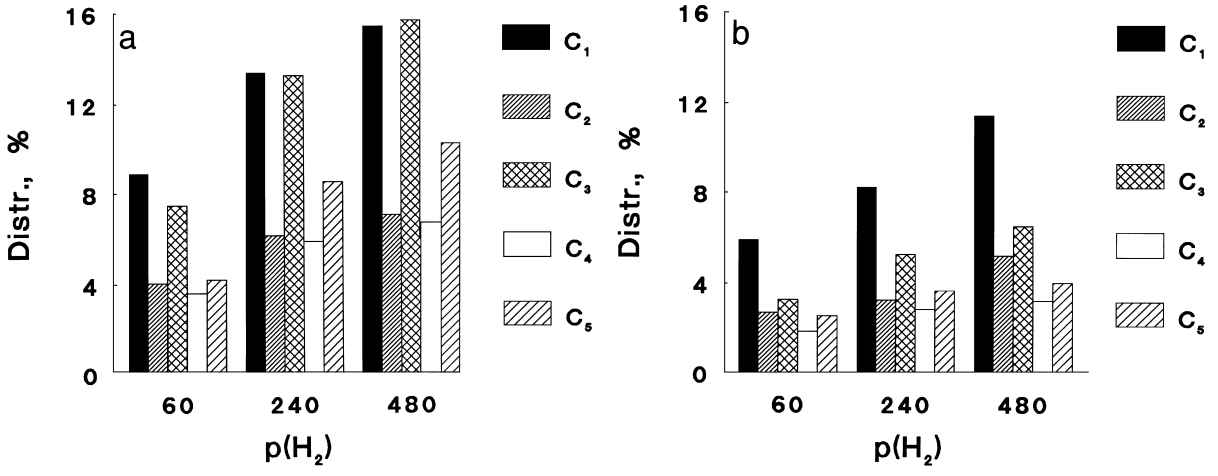

FIG. 6. Fragment distribution from *n*-hexane (normalized to Σ products = 100%) at three different hydrogen pressures. $T = 603$ K. (a) Catalyst **T**. (b) Catalyst **N**.

a maximum as a function of $p(H_2)$; otherwise, no dramatic changes were observed in the hydrogen pressure sensitivities of the selectivity of other products compared with the low-temperature plots (cf. Figs. 3 and 5). The differences between the two temperatures can be attributed, in part, to the enhanced thermodynamic stability of olefins.

DISCUSSION

The differences between catalytic properties can be evaluated in terms of a general mechanism accepted for reactions over supported metals (34). At 603 K the catalysts that we studied can be considered as monofunctional metallic catalysts because the metallic function is active above 473 K but the acidic one only above 673 K (39). Thus, metal-catalyzed isomerization reactions [via a C_5-cyclic or a bond shift route (40)], metal-catalyzed aromatization by 1–6 ring closure (41), and hydrogenolysis should be considered. Metal-catalyzed aromatization probably involves open-chain unsaturated intermediates (41, 42) and requires ensembles of three Pt atoms of triangular symmetry (15, 34, 41). C_5 ring closure and ring opening to isomers are related reactions involving the same surface intermediate probably attached to two Pt atoms (34, 41). Surface hydrogen availability would determine whether this intermediate desorbs as methylcyclopentane or reacts further to isomers (34, 35, 43). Hydrogenolysis is likely to require ensembles of several Pt atoms (44) which, according to some studies, should have a particular arrangement (B_5 sites) (45). Single internal rupture is characteristic of Pt (34, 46) but some multiple rupture is superimposed over it, especially if the catalyst is fresh and free from carbonaceous deposits (35, 47). It cannot be excluded that this multiple rupture occurs on single atom sites (perhaps corners) active in a rich hydrogen environment (35, 47, 48).

TABLE 4

Selectivity of *n*-Hexane Reaction at Various Sampling Times[a]

Catalyst	Sampling time (min)	Conversion (%)	Product selectivity (%)				
			$<C_6$	Isomer	MCP	Olefin	Benzene
PT	5	7	17	24	42	2	15
	93	46	27	30	25	1	17
	230	74	27	31	24	1	17
PN	5	8	15	31	36	1	17
	100	61	25	35	17	1	22
	295	86	36	31	8	~0	25
T	5	17	15	24	40	2	19
	100	65	31	32	14	1	22
N	5	9	8	21	50	5	16
	100	44	14	35	31	1	19

[a] $T = 603$ K, $p(nH) : p(H_2) = 10 : 120$.

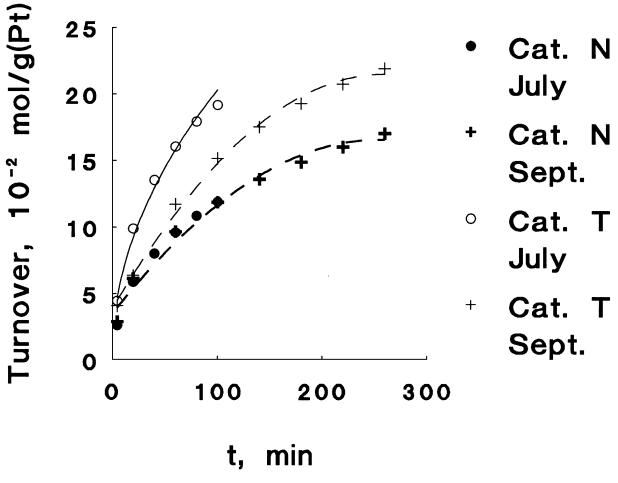

FIG. 7. Long-term stability of bimetallic catalysts. $T = 603$ K.

TABLE 5

Selectivity of *n*-Hexane Reaction after Several Regenerations[a]

Catalyst	No. of regenerations	Conversion (%)	Product selectivity (%)				
			$<C_6$	Isomer	MCP	Olefin	Benzene
T	0	30	31	22	28	1	18
	6	19	16	24	39	2	19
	14	15	12	25	43	2	18
	32	12	9	25	48	1	17
N	0	13	12	20	45	4	19
	6	10	8	21	51	4	16
	14	9	8	23	51	2	16
	32	9	9	23	50	1	17

[a] $T = 603$ K, $p(nH) : p(H_2) = 10 : 120$, sampling time = 5 min.

The overall and specific activities of EUROPT-1 were lower than those of any Pt/Al_2O_3 catalysts of the present study (Figs. 1 and 2). EUROPT-1 showed an inherent ability to catalyze, first, nondegradative skeletal reactions of *n*-hexane, the formation of methylcyclopentane (MCP) as well as skeletal isomers being favored (35, 37). The selectivities obtained in our experiments are in good agreement with the results published earlier (35, 37, 47). Indeed, hydrogenolysis selectivities on both monometallic Pt/Al_2O_3 catalysts (Fig. 3) were much higher than those observed on EUROPT-1. We attribute the lower total activity of EUROPT-1 to hindered hydrogenolysis over this catalyst, due, perhaps, to its particular geometry (37), exhibiting a lower abundance of sites claimed to be active for hydrogenolysis, incomplete edge or corner moieties (B_5 sites) (45), as well as the low abundance of single-atom corner sites (47, 48). This finding can be used as evidence that dispersion alone cannot determine catalytic activity and/or selectivity. This statement does not involve the assumption of any metal–support interaction, although such effects are not excluded.

The poor dispersion of sample **PN** can be attributed to the self-reduction of Pt by interaction with the NH_3 ligands, resulting in highly mobile intermediates. On the other hand, the higher molar ratio of Cl to Pt in H_2PtCl_6, the precursor of **PT**, renders the formation of Pt–O–Cl species possible. Those have been reported to be active in Pt redispersion on alumina (49). The sample **PN** behaves as one expects from a catalyst exposing large contiguous Pt islands; i.e., it promotes reactions requiring multiatom ensembles, such as hydrogenolysis and aromatization (Fig. 3).

Catalyst **N** showed crystallites mainly in the range 10–30 Å with few units of about 150 Å (as seen by electron microscopy) and no diffraction corresponding to any tin oxide was present (50). *Ex situ* X-ray diffraction showed the appearance of PtSn alloy (33b). *In situ* EXAFS indicated that PtSn was stabilized at higher temperatures in an H_2 atmosphere only (51). Air treatment from 270°C led to oxidation of a part of the Sn. Repeated reduction restored some of the PtSn alloy structure, but the tin oxide that migrated out of the Pt clusters was lost to the bimetallic particles (51). Since EXAFS indicated that each Pt atom had in the nearest neighborhood more Pt atoms than corresponded to a pure stoichiometric PtSn phase after reduction, the particles in catalyst **N** should consist of a solid solution of Sn in Pt, stable up to 8 at.% Sn (18), plus PtSn. Sn oxidized by contact with O_2 during regeneration should also be present as separate SnO_2 particles. The catalytic properties should be attributed to Pt sites interacting with those nonplatinum entities.

We assumed a better distribution of Sn in catalyst **N** on the basis of our previous publication (32). Let us discuss to what extent the present results confirm our preliminary conclusions, considering any possible electronic interactions between Pt and Sn as well as the structural model outlined above.

The overall activity of $Pt–Sn/Al_2O_3$ catalysts was lower than that of Pt/Al_2O_3 catalysts, due to the loss of some surface Pt atoms (52, 53). Tin should have been enriched to a larger extent on catalyst **N**: in this case the dispersion of Pt is smaller (18.3%) than with catalyst **T** (60.6%), both having close to nominal Pt and Sn content (Table 1).

The turnover frequency of catalyst **N** is higher than that of catalyst **T**. We assume that Pt atoms in the Pt–Sn ensembles in catalyst **N** keep their Pt-like activity to a greater extent than in catalyst **T**. By stating this, we do not wish to attribute any definite structure to "Pt–Sn ensembles" or define "active sites" in any of the catalysts.

The selectivity pattern changed profoundly with bimetallic samples. The number of larger Pt ensembles required for hydrogenolysis (44) is obviously smaller on $Pt–Sn/Al_2O_3$ catalysts than on Pt/Al_2O_3 catalysts, thus confirming the diluting effect mentioned. Of the two $Pt–Sn/Al_2O_3$ samples, catalyst **N** has the lower hydrogenolysis activity and this confirms the smaller number of contiguous Pt islands as a consequence of this method of preparation. The fragment patterns of Fig. 6 indicate that catalyst **N** with lower hydrogenolysis ability produced throughout more methane. Attributing this excess CH_4 to multiple rupture on single atom sites (48), the apparent contradiction disappears. Note that this additional multiple fragmentation occurred also on EUROPT-1 with sufficient hydrogen present (35), although EUROPT-1 otherwise exhibited an exceptionally low fragmentation selectivity (37).

The higher selectivity of aromatization at low hydrogen pressures over the Pt catalysts indicates the possible importance of unsaturated intermediates and the stepwise aromatization pathway (41). The inferior aromatization activity of catalyst **N** compared with catalyst **PN** can be due to the same reason: its tin content reduces the number of three-Pt-atom ensembles for aromatization of *n*-hexane (16). One has to

recall the results that much greater amounts of hexadienes appeared in the gas phase as intermediates of aromatization with Pt–Sn/Al_2O_3 than with Pt/Al_2O_3, indicating the lesser ability of their further reaction to benzene (without desorption) on the bimetallic catalyst (54).

The increase in benzene selectivity at the expense of olefins agrees with the assumed pathway of the primary product hexenes reacting to aromatics (42, 43). This is naturally more pronounced at 663 K (Figs. 8 and 9). Sample **PN**, with the largest particles, seems to be the most active in this process. The aromatization selectivity of catalyst **T** is not inferior to that of catalyst **PT**, at both temperatures studied. (Table 4 and Fig. 9). In this case the more roughly distributed tin in **T** apparently did not decrease significantly the number of active ensembles for aromatization.

At higher hydrogen pressures hydrogen-richer intermediates of C_6 saturated products become preferred. Assuming a prevailing C_5-cyclic mechanism for skeletal isomerization over all catalysts (40, 43, 55), the amount of available surface hydrogen should determine the isomer/C_5-cyclic ratio, more hydrogen favoring isomerization. The cyclic pathway is a typically metal-catalyzed reaction. The ratio of 2,3-DMB to the sum of methylpentanes was found to be characteristic of the relative importance of acid- and metal-catalyzed isomerization pathways (56). The cooperation of an acidic and metallic site should result in higher 2,3-DMB/ΣMP ratios (57, 58). The values in Table 2 are close to those observed over the totally acid-free EUROPT-1. The somewhat higher values measured at 663 K may indicate the commencement of the bifunctional mechanism at this temperature with some deactivation of the metallic sites. The higher Cl content of sample **T** does not result in a larger amount of isomers or more dimethylbutane. Hence the acidic isomerization pathway does not seem to be too important, perhaps because Sn ions were found to poison the strong acidic support sites active in isomerization (25). The ratio 2-MP/3-MP should be close ot the statistical value of 2 expected from a random opening of the proposed surface intermediate, methylcyclopentane, on metallic sites (35). Indeed, the actual values approach and even exceed this number (Table 3). Both values show a hydrogen pressure dependence, random ring opening reactions being less pronounced at low hydrogen pressures. This was attributed to metal–acid cooperation on Pt/zeolites (58) and to carbonization commencing on EUROPT-1 (35). With less hydrogen available, the metal surface of the catalyst contains, indeed, more unsaturated intermediates hard to remove. These species compete with the common surface intermediate of isomers plus MCP for surface hydrogen (43). The formation of olefins is enhanced and that of MCP and isomers suppressed because of the lack of available hydrogen at the lowest $p(H_2)$ values.

The higher selectivity of C_5-cyclic reactions on catalyst **N** (observed with longer runs, too, Table 4) agrees well with the two-atom ensembles proposed for this reaction as opposed to aromatization on three Pt atoms (15). This would contradict the assumption of aromatization on single-atom sites (9). The somewhat higher aromatization selectivity of monometallic catalysts can also be due to the larger Pt islands being more active also in hydrogenolysis (Table 4). The higher dehydrogenation activity of catalyst **N** (Figs. 3, 5 and 9) compared with Pt/Al_2O_3 and catalyst **T** can also be attributed to a better Pt distribution, i.e., more single Pt atoms between Sn atoms (11).

This means that catalyst **N** "inherits" the intimate contact of Pt and Sn atoms (one each in each precursor molecule). Previous results (32) are in line with the proposal of its single Pt sites interacting electronically with Sn atoms (9). The structure of catalyst **T**, in turn, can be visualized as consisting of PtSn areas as well as pure Pt islands, the latter being responsible for the high initial hydrogenolysis selectivity. Its long-term loss of activity (Fig. 7, Table 5) may be attributed

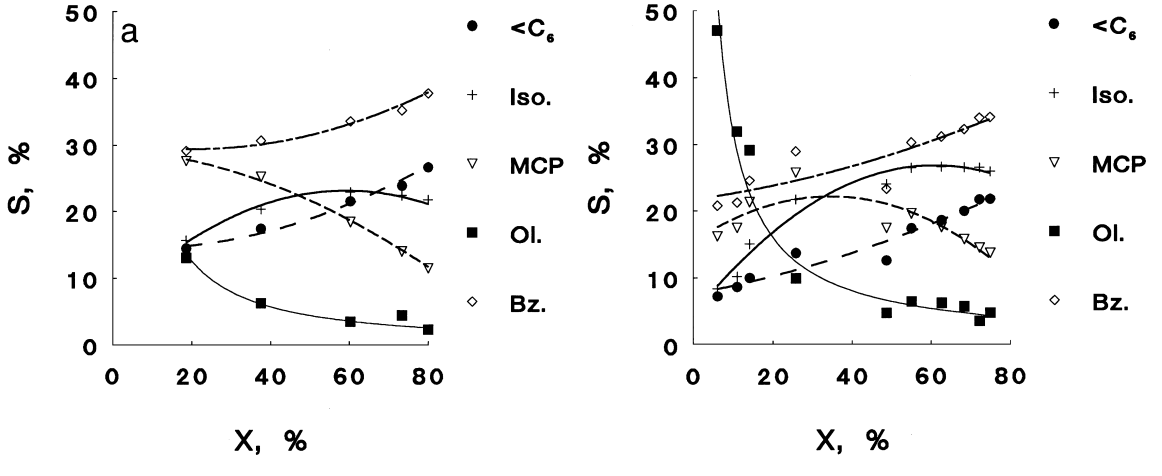

FIG. 8. Selectivity of individual product groups (S) as a function of overall conversion (X). $T = 663$ K, $p(nH) = 10$ Torr, $p(H_2) = 120$ Torr. (a) Catalyst **T**. (b) Catalyst **N**.

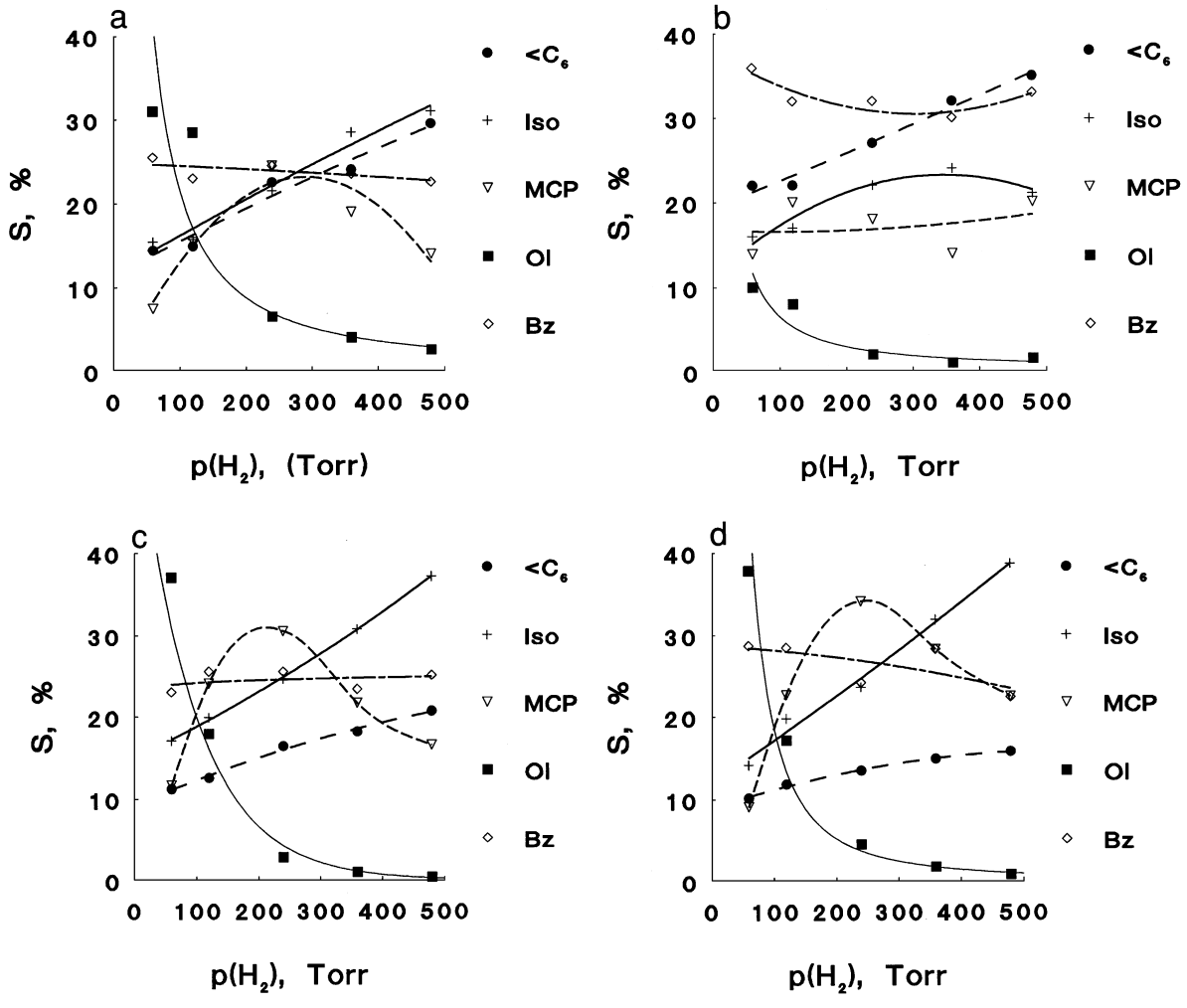

FIG. 9. Selectivities of individual products from *n*-hexane as a function of the hydrogen pressure at $T = 663$ K. (a) Catalyst **PT** ("traditional" Pt/Al_2O_3). Overall conversions: ~5% at $p(H_2) = 60$ Torr, ~11 to ~23% at higher hydrogen pressures. (b) Catalyst **PN** ("new" Pt/Al_2O_3). Overall conversions: ~4% at $p(H_2) = 60$ Torr, ~9 to ~26% at higher hydrogen pressures. (c) Catalyst **T** ("traditional" $Pt–Sn/Al_2O_3$). Overall conversions: ~14% at $p(H_2) = 60$ Torr, ~20 to ~42% at higher hydrogen pressures. (d) Catalyst **N** ("new" $Pt–Sn/Al_2O_3$). Overall conversions: ~9% at $p(H_2) = 60$ Torr, ~11 to ~28% at higher hydrogen pressures.

to irreversible coke accumulation or to a gradual accumulation of SnO_2 (produced during subsequent regenerations) on these Pt-rich areas. Although the *number* of active sites may have decreased, their *nature* does not change during this process, as evidenced by the decreasing activity and rather stable selectivity values in Table 5.

All the catalytic results can be explained adequately by the geometric model, by assuming a dilution of the Pt ensembles by Sn, without making assumptions on the state of Sn (solid solution or alloy). The Joyner–Shpiro model, in turn, is based on an electronic interaction between a clean Pt surface and a sublayer rich in Sn. Such interactions should lead to $Pt^{\delta+}$ surface entities with decreased hydrogen adsorption ability. Passos *et al.* (59) reported, indeed, a lower hydrogen chemisorption capacity for $Pt–Sn/Al_2O_3$ catalysts as compared with Pt/Al_2O_3 and they explained butane hydrogenolysis results by the geometric model. The ample amounts of formation of C_6 saturated products at the expense of hydrogenolysis and aromatization in the present study indicated a larger amount of available sites for C_6 saturated formation on bimetallic samples. It remains an open question whether it is due to the availability of more hydrogen on these catalysts or just to their more favorable sites for this reaction.

Long-term deactivation (activity drop) was accompanied by a much smaller shift in selectivities with both catalysts. The most marked shift was the hampering of fragmentation and a gain in methylcyclopentane formation without too much of an effect on benzene formation (Table 5). This shows again that the number of active sites may have changed more markedly than their nature. Of the two $Pt–Sn/Al_2O_3$ samples, further transformation of

methylcyclopentane to skeletal isomers during a long run is more marked on catalyst **T**. This may be the only indication that the more pronounced Pt–Sn interactions may have decreased the surface hydrogen concentration on sample **N** since, of all processes studied, this reaction would demand the most hydrogen (36). This difference is observed even after several deactivation/regeneration cycles (Table 5).

CONCLUSIONS

1. Adding tin to Pt/Al_2O_3 decreases the overall activity in hexane reactions and increases somewhat the turnover frequency. It also modifies the selectivities: hydrogenolysis activity of $Pt–Sn/Al_2O_3$ catalysts is much lower, while selectivity of isomerization and methylcyclopentane formation is higher.

2. Hydrogen effects are similar on all catalysts (except for **N**): higher H_2 pressures usually favor hydrogenolysis, promote C_5-cyclic reactions, and suppress dehydrogenation, and, to some extent, aromatization.

3. Hydrogenolysis and aromatization are less marked, on catalyst **N**, and dehydrogenation and isomerization are more pronounced than on catalyst **T**, mainly due to a better dispersion of Sn. The differences in fragment distribution could also be interpreted in these terms.

4. Aromatization is more marked at 663 K; at the same time, the low hydrogenolysis selectivity of bimetallic catalysts is preserved, especially with sample **N**. The monometallic catalyst prepared from the same precursor as **N** (catalyst **PN**) has the lowest dispersion and highest aromatization selectivity.

5. Catalyst **N** also had better long-term stability, the product distribution over catalyst **T** approaching slowly the values observed over sample **N**. This could have been due to the deactivation of the pure Pt areas in sample **T**.

6. All activity and selectivity changes can be rationalized in terms of geometric (ensemble) effects, with Sn as a solid solution in Pt or as a PtSn alloy diluting multiatomic Pt sites. This statement does not exclude electronic Sn–Pt interactions; such a phenomenon was assumed on catalyst **N** (32).

ACKNOWLEDGMENTS

The work was started in the framework of CNRS–HAS cooperation (No. 4.2) and was completed with the support of the French–Hungarian Technical Cooperation (Balaton Program 96015). The authors thank Mr. Karoly Matusek for carrying out selective chemisorption measurements for catalyst characterization.

REFERENCES

1. Ponec, V., and Bond, G. C., "Catalysis by Metals and Alloys," Stud. Surf. Sci. Catal., Vol. 95. Elsevier, Amsterdam, 1995.
2. Murthy, K. R., Sharma, N., and George, N., *in* "Catalytic Naptha Reforming" (G. J. Antos, A. M. Aitani, and J. M. Parera, Eds.), p. 207. Marcel Dekker, New York, 1995; Boitiaux, J. P., Deves, J. M., Didillon, B., and Marcilly, C. R., ibid., p. 79.
3. Sachtler, W. M. H., *J. Mol. Catal.* **25**, 1 (1984).
4. Clarke, J. K. A., *Chem. Rev.* **75**, 391 (1975).
5. Sachtler, W. M. H., and van Santen, R. A., *in* "Advances in Catalysis" (H. Pines, D. D. Eley, and P. B. Weisz, Eds.), Vol. 26, p. 69. Academic Press, New York, 1977.
6. Guczi, L., *J. Mol. Catal.* **25**, 13 (1984).
7. Guczi, L., and Sárkány, A., *in* "Catalysis, Specialists Periodical Reports" (J. J. Spivey and S. K. Agarwal, Eds.), Vol. 11, p. 318. Roy. Soc. of Chem., London, 1994.
8. Davis, B. H., Westfall, G. A., Watkins, J., and Pezzanite, J., *J. Catal.* **42**, 247 (1976).
9. Coq, B., and Figueras, F., *J. Catal.* **85**, 197 (1984).
10. Burch, R., *J. Catal.* **71**, 348 (1981).
11. Burch, R., and Garla, L. C., *J. Catal.* **71**, 360 (1981).
12. Burch, R., *Catal. Today* **10**, 233 (1991).
13. Parera, J. M., Beltramini, J. N., Querini, C. A., Martinelli, E. E., Churin, E. J., Aloe, P. E., and Figoli, N. S., *J. Catal.* **99**, 39 (1986).
14. Palazov, A., Bonev, C., Shopov, D., Leitz, G., Sárkány, A., and Völter, J., *J. Catal.* **103**, 249 (1987).
15. Biloen, P., Helle, J. N., Verbeek, H., Dautzenberg, F. M., and Sachtler, W. M. H., *J. Catal.* **63**, 112 (1980).
16. Dautzenberg, F. M., Helle, J. N., Biloen, P., and Sachtler, W. M. H., *J. Catal.* **63**, 119 (1980).
17. Biloen, P., Dautzenberg, F. M., and Sachtler, W. M. H., *J. Catal.* **50**, 77 (1977).
18. Hanson, M., and Anderko, K., "Constitution of Binary Alloys," p. 1141. McGraw–Hill, New York, 1958.
19. Adkins, S. R., and Davis, B. H., *J. Catal.* **89**, 371 (1984).
20. Sexton, B. A., Hughes, A. E., and Foger, K., *J. Catal.* **88**, 466 (1984).
21. Balakrishnan, K., and Schwank, J., *J. Catal.* **127**, 287 (1991).
22. Li, Y. X., Stencel, J. M., and Davis, B. H., *React. Kinet. Catal. Lett.* **37**, 273 (1988).
23. Li, Y. X., Stencel, J. M., and Davis, B. H., *Appl. Catal.* **64**, 71 (1990).
24. Srinivasan, R., De Angeles, J., and Davis, B. H., *J. Catal.* **106**, 449 (1987).
25. Bacaud, R., Bussière, P., and Figueras, F., *J. Catal.* **69**, 399 (1981).
26. Berndt, H., Mehner, H., Völter, J., and Meisel, W., *Z. Anorg. Allg. Chem.* **429**, 47 (1977).
27. Kuznetsov, V. I., Belyi, A. S., Yurchenko, E. N., Smolikov, M. A., Protasova, M. T., Zatolokina, E. V., and Duplyakin, V. K., *J. Catal.* **99**, 159 (1986).
28. Vértes, C., Tálas, E., Czakó-Nagy, I., Ryczkowski, J., Göbölös, S., Vértes, A., and Margitfalvi, J., *Appl. Catal.* **68**, 149 (1991).
29. Srinivasan, R., and Davis, B. H., *Appl. Catal. A* **87**, 45 (1992).
30. Lieske, H., and Völter, J., *J. Catal.* **90**, 96 (1984).
31. Joyner, R. W., and Shpiro, E. S., *Catal. Lett.* **9**, 239 (1991).
32. Kappenstein, C., Saouabe, M., Guérin, M., Marécot, P., Uszkurat, I., and Paál, Z., *Catal. Lett.* **31**, 9 (1995).
33. (a) El Biyyadh, A., Guérin, M., Kappenstein, C., Bazin, D., and Dexpert, H., *J. Chim. Phys.* **86**, 1751 (1989). (b) El Abed, A., El Quebbaj, S., Guérin, M., Kappenstein, C., Saouabe, M., and Marécot, P., *J. Chim. Phys.* **92**, 1307 (1995). (c) Lázár, K., Matusek, K., Kappenstein, C., Guérin, M., and Paál, Z., in preparation.
34. Paál, Z., *in* "Catalytic Naphtha Reforming" (G. J. Antos, A. M. Aitani, and J. M. Parera, Eds.), p. 19. Marcel Dekker, New York, 1995.
35. Paál, Z., Groeneweg, H., and Paál-Lukács, J., *J. Chem. Soc. Faraday Trans.* **86**, 3159 (1990).
36. Paál, Z., *Catal. Today* **12**, 297 (1992).
37. Bond, G. C., and Paál, Z., *Appl. Catal. A* **86**, 1 (1992).
38. Margitfalvi, J., Szedlacsek, P., Hegedüs, M., and Nagy, F., *Appl. Catal.* **15**, 69 (1985).
39. Corolleur, C., Gault, F. G., Juttard, D., Maire, G., and Muller, J. M., *J. Catal.* **21**, 250 (1971).

40. Amir-Ebrahimi, V., and Gault, F. G., *J. Chem. Soc. Faraday Trans. 1* **76**, 1735 (1980).
41. Paál, Z., *in* "Advances in Catalysis" (H. Pines, D. D. Eley, and P. B. Weisz, Eds.), Vol. 29, p. 273. Academic Press, New York, 1980.
42. Paál, Z., and Tétényi, P., *J. Catal.* **30**, 350 (1973).
43. Paál, Z., Xu, X. L., Paál-Lukács, J., Vogel, W., Muhler, M., and Schlögl, R., *J. Catal.* **152**, 252 (1995).
44. Anderson, J. R., *in* "Advances in Catalysis" (H. Pines, D. D. Eley, and P. B. Weisz, Eds.), Vol. 23, p. 1. Academic Press, New York, 1973.
45. Dauscher, A., Garin, F., and Maire, G., *J. Catal.* **105**, 233 (1987).
46. Paál, Z., and Tétényi, P., *Nature* **267**, 234 (1977).
47. Paál, Z., Manninger, I., Zhan, Zh., and Muhler, M., *Appl. Catal.* **66**, 305 (1990).
48. Anderson, J. B. F., Burch, R., and Cairns, J. A., *J. Catal.* **107**, 364 (1987).
49. Lieske, H., Lietz, G., Spindler, H., and Völter, J., *J. Catal.* **81**, 8 (1983).
50. Saouabe, M., Thesis, No. 542, Université de Poitiers, 1992.
51. El Abed, A., El. Qebbaj, S. E., Guérin, M., Kappenstein, C., Dexpert, H., and Villain, F., *J. Chim. Phys.* **94**, 54 (1997).
52. Bouwman, R., Toneman, L. H., and Holscher, A. A., *Surf. Sci.* **35**, 8 (1973).
53. Verbeek, H., and Sachtler, W. M. H., *J. Catal.* **42**, 257 (1976).
54. Paál, Z., Dobrovolszky, M., Völter, J., and Lietz, G., *Appl. Catal.* **14**, 33 (1985).
55. Zimmer, H., Dobrovolszky, M., Tétényi, P., and Paál, Z., *J. Phys. Chem.* **90**, 4758 (1986).
56. Carvill, B. T., Lerner, B. A., Adelman, B. J., Tomczak, D. C., and Sachtler, W. M. H., *J. Catal.* **144**, 1 (1993).
57. Zhan, Zh., Manninger, I., Paál, Z., and Barthomeuf, D., *J. Catal.* **147**, 333 (1994).
58. Paál, Z., Zhan, Zh., Manninger, I., and Sachtler, W. M. H., *J. Catal.* **155**, 43 (1995).
59. Passos, F. B., Schmal, M., and Vannice, M. A., *J. Catal.* **160**, 106 (1996).